PHYSICAL REVIEW D VOLUME 52, NUMBER 1 1 JULY 1995

Multiple gluon effects in fermion-(anti)fermion scattering at and beyond CERN LHC energies

D. B. DeLaney, S. Jadach,* Ch. Shio, G. Siopsis, and B. F. L. Ward

Department of Physics and Astronomy, The University of Tennessee, Knoxville, Tennessee 37996-1200

(Received 22 February 1994)

We extend the methods of Yennie, Frautschi, and Suura (YFS) to compute, via Monte Carlo methods, the effects of multiple gluon emission in the processes $q+\overset{(-)}{q}{}' \to q''+\overset{(-)}{q}{}''' + n(G)$, where G is a soft gluon. We show explicitly that the infrared singularities in the respective simulations are canceled to all orders in α_s. Some discussion of this result from the standpoint of confinement is given. More importantly, we present, for the first time, sample numerical Monte Carlo data on multiple soft gluon emission in the rigorously extended YFS framework. We find that such soft gluon effects must be taken into account for precise physics simulations at and beyond CERN LHC energies.

PACS number(s): 13.85.−t, 11.55.−m, 12.38.Cy, 14.70.Dj

I. INTRODUCTION

Now that the CERN Large Hadron Collider (LHC) is approved, is in its early stages of development, and continues to gain momentum, it becomes more and more necessary to prepare for the physics exploration which the LHC and possible near-term upgrades will provide. The primary issue in this exploration is the comparison between predictions from the standard $\mathrm{SU}(2)_L \otimes \mathrm{U}(1) \otimes \mathrm{SU}(3)_C$ theory and its possible extensions, and what will be observed by the ATLAS and CMS Collaborations, with the discovery of the Higgs particle or whatever it represents as of course a primary goal of such comparisons. Thus, it is important to know the theoretical predictions as accurately as is necessary to exploit the expected detector performances of ATLAS and CMS to the fullest extent. In particular, higher order radiative corrections to these predictions (due to multiple-photon and multiple-gluon effects) are in fact essential to obtain the proper precision on the signal and background processes in the respective LHC environment. In [1], we have developed Yennie-Frautschi-Suura [2] (YFS) multiphoton Monte Carlo event generators for calculating $n\gamma$ effects in LHC processes. In what follows, we now develop the extension of our own YFS Monte Carlo–based higher order radiative correction methods to multiple-gluon effects in LHC processes. Such a calculation of $n(G)$ effects has not appeared elsewhere, where we use G to denote a gluon.

More precisely, we want to use the fact that, by the uncertainty principle, infinite-wavelength gluons should not affect the motion of quarks and gluons inside a proton, whose radius is $\sim$ 1 fm. Thus, we have recently realized [3] this physical requirement in perturbation theory by showing that in our prototypical processes $q+\overset{(-)}{q}{}' \to q''+\overset{(-)}{q}{}''' + (G)$, the infrared singularities cancel at $O(\alpha_s)$, just as they cancel in the analogous QED process $f + f' \to f + f' + \gamma$. We then are able to define the QCD analogues of the famous YFS infrared functions [2] B and $\tilde{B}$ which describe the virtual and real infrared singularities in QED processes to all orders in α. These functions B_{QCD} and $\tilde{B}_{\mathrm{QCD}}$ then describe the infrared singularities in QCD in the processes $q+\overset{(-)}{q}{}' \to q''+\overset{(-)}{q}{}''' + n(G)$ to all orders in α_s. The sum $B_{\mathrm{QCD}} + \tilde{B}_{\mathrm{QCD}}$ is infrared finite and allows us to extend our YFS Monte Carlo methods, widely used in SLAC Linear Collider (SLC) or CERN e^+e^- collider LEP physics for higher order QED radiative effects, to the analogous Monte Carlo methods in QCD processes for the physics objectives of the LHC and possible future higher energy hadron colliders. We call the resulting programs LHCYFSG and LHCBHLG, for they are the QCD extensions of the QED $n\gamma$ Monte Carlo's SSCYFS2 and LHCBHL. Here we recall that SSCYFS2 was already described in [1] and LHCBHL is the analogous LHC extension of the YFS Monte Carlo BHLUMI 2.01 [4] for the SLC or LEP luminosity process $e^+e^- \to e^+e^- + n\gamma$.

In what follows, we shall present sample Monte Carlo data for the process $q+\overset{(-)}{q}{}' \to q''+\overset{(-)}{q}{}''' + n(G)$ from the event generator LHCBHLG. Analogous results from LHCYFSG will appear elsewhere [5]. The latter Monte Carlo only simulates initial-state gluon radiation, whereas LHCBHLG simulates initial-state and final-state n-gluon radiation, as well as the respective initial-final-state interference effects. Further, we emphasize that (unlike BHLUMI 2.01) LHCBHLG is not restricted to small scattering angles. Note finally that LHCYFSG is an initial-state restriction of LHCBHLG and hence is useful for cross-checking our work.

Our work is organized as follows. In the next section, we derive the extension of the YFS exponentiation to n-gluon emission and the attendant extension of SSCYFS2 and LHCBHL. In Sec. III, we present sample Monte

*Permanent address: Institute of Nuclear Physics, ul. Kawiory 26a, Cracow, Poland.

Carlo data for n-gluon emission for the CMS, ATLAS, Solenoidal Detector Collaboration (SDC), and Gamma-Electron-Muon (GEM) Collaboration acceptances. Section IV contains some concluding remarks. The Appendix contains some technical details.

II. INFRARED SINGULARITY CANCELLATION IN QCD

In this section, we derive the analogue of the YFS infrared functions B and $\tilde{B}$ for QCD, $B_{\rm QCD}$ and $\tilde{B}_{\rm QCD}$, for the process $q+\overset{(-)}{q}{}' \to q''+\overset{(-)}{q}{}''' + (G)$. We will focus on the case of most interest to us, in which a gluon is exchanged in the t channel and we require that the exchanged gluon carries large momentum transfer so that the outgoing quark (antiquark) is in the $|\eta| \le 2.8$ acceptance of the CMS, ATLAS, and SDC (and GEM). This situation is depicted in Fig. 1. We remark that if the relevant exchange is a color-singlet exchange (such as W or Z^0 exchange), we can obtain the corresponding formulas for $B_{\rm QCD}$ and $\tilde{B}_{\rm QCD}$ by dropping the terms in the color-exchange case which arise from noncommutativity of the respective QCD λ^a matrices in the relevant quark representation.

Specifically, following the kinematics in Fig. 1(a), we note that, for the CMS, ATLAS, SDC, and GEM acceptance, we always have $-Q^2 = -(q_1-q_2)^2 \gg \Lambda^2_{\rm QCD}$, so that perturbative QCD methods are applicable. What we wish to do is to extract the infrared-singular part of the $O(\alpha_s)$ amplitude in Fig. 1(b), in complete analogy with the YFS [2] extraction of the infrared-singular portion of the analogous amplitude in QED via the famous YFS virtual infrared function B. To this end, we first note that, by explicit calculation, the graphs (v)–(vii) are not infrared divergent (we compute the gluon vacuum polarization to order α_s as well), so that the infrared-singular part of Fig. 1(b) is given by just the same graphs as the infrared-singular part of the analogous process in QED. We follow the YFS methods in [2] and find the infrared-singular part of Fig. 1(b) to be given by

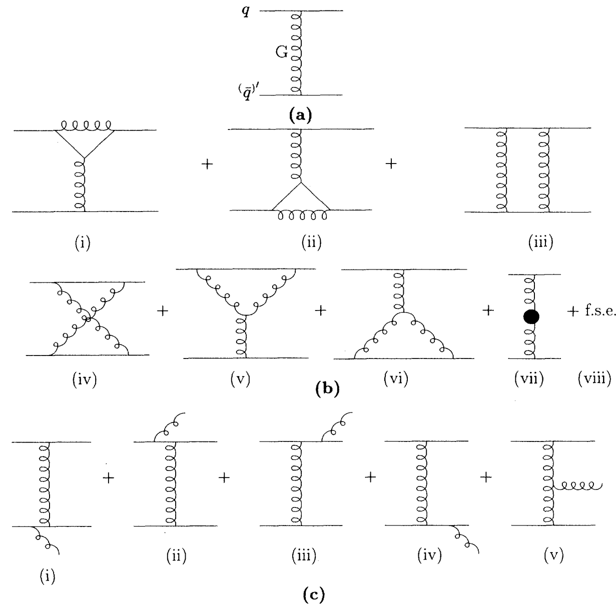

FIG. 1. The process $q+\overset{(-)}{q}{}' \to q+\overset{(-)}{q}{}'+(G)$ to $O(\alpha_s)$: (a) Born approximation; (b) $O(\alpha_s)$ virtual correction; (c) $O(\alpha_s)$ bremsstrahlung process. Here, f.s.e. represents the fermion self-energies.

$$\mathcal{M}_{v,\rm IR} = \alpha_s B_{\rm QCD}\mathcal{M}_{8B} + \alpha_s \bar{B}_{\rm QCD}\mathcal{M}_{0B} \ , \tag{1}$$

where $\mathcal{M}_{8B}$ is the respective Born amplitude in Fig. 1(a) and where

$$\begin{aligned}
B_{\rm QCD} = \frac{i}{(8\pi^3)}\int \frac{d^4k}{(k^2-\lambda^2+i\epsilon)}\Bigg[& C_F\left(\frac{2p_1+k}{k^2+2k\cdot p_1+i\epsilon}+\frac{2p_2-k}{k^2-2k\cdot p_2+i\epsilon}\right)^2 \\
& +\Delta C_s\frac{2(2p_1+k)\cdot(2p_2-k)}{(k^2+2k\cdot p_1+i\epsilon)(k^2-2k\cdot p_2+i\epsilon)}+C_F\left(\frac{2q_1+k}{k^2+2k\cdot q_1+i\epsilon}-\frac{2q_2-k}{k^2-2k\cdot q_2+i\epsilon}\right)^2 \\
& +\Delta C_s\frac{2(2q_1+k)\cdot(2q_2-k)}{(k^2+2k\cdot q_1+i\epsilon)(k^2-2k\cdot q_2+i\epsilon)}+C_F\left(\frac{2p_2+k}{k^2+2k\cdot p_2+i\epsilon}-\frac{2q_2+k}{k^2+2k\cdot q_2+i\epsilon}\right)^2 \\
& -\Delta C_t\frac{2(2q_2+k)\cdot(2p_2+k)}{(k^2+2k\cdot q_2+i\epsilon)(k^2+2k\cdot p_2+i\epsilon)}+C_F\left(\frac{2p_1+k}{k^2+2k\cdot p_1+i\epsilon}-\frac{2q_1+k}{k^2+2k\cdot q_1+i\epsilon}\right)^2 \\
& -\Delta C_t\frac{2(2q_1+k)\cdot(2p_1+k)}{(k^2+2k\cdot q_1+i\epsilon)(k^2+2k\cdot p_1+i\epsilon)}-C_F\left(\frac{2p_1+k}{k^2+2k\cdot p_1+i\epsilon}-\frac{2q_2+k}{k^2+2k\cdot q_2+i\epsilon}\right)^2 \\
& +\Delta C_u\frac{2(2p_1+k)\cdot(2q_2+k)}{(k^2+2k\cdot p_1+i\epsilon)(k^2+2k\cdot q_2+i\epsilon)}-C_F\left(\frac{2q_1+k}{k^2+2k\cdot q_1+i\epsilon}-\frac{2p_2+k}{k^2+2k\cdot p_2+i\epsilon}\right)^2 \\
& +\Delta C_u\frac{2(2q_1+k)\cdot(2p_2+k)}{(k^2+2k\cdot q_1+i\epsilon)(k^2+2k\cdot p_2+i\epsilon)}\Bigg]
\end{aligned} \tag{2}$$

with $C_F = 4/3$ = quadratic Casimir invariant of the quark color representation, λ equal to the standard infrared regulator mass [6] and

$$\Delta C_s = \begin{cases} -1, & qq' \text{ incoming}, \\ -1/6, & q\bar{q}' \text{ incoming}, \end{cases}$$

$$\Delta C_t = -3/2,$$

and

$$\Delta C_u = \begin{cases} -5/2, & qq' \text{ incoming}, \\ -5/3, & q\bar{q}' \text{ incoming}. \end{cases} \tag{3}$$

Thus, we see that the non-Abelian nature of QCD causes $\Delta C_j \neq 0$.

The additional term in (1), which arises from color algebra, consists of what we call the "singlet" exchange Born amplitude which is obtained from Fig. 1(a) by substituting λ^0 for the color matrices λ^a, where $\lambda^0 \equiv I/\sqrt{6}$. The corresponding value of $\bar{B}_{\rm QCD}$ in (1) is obtained from (2) by setting $C_F \equiv 0$ and $\Delta C_t = 0$ in (2) and by setting

$$\Delta C_u = \Delta C_s = \begin{cases} -C_F, & qq' \text{ incoming}, \\ C_F, & q\bar{q}' \text{ incoming}, \end{cases} \tag{4}$$

in (2). We note that, to order α_s, the "singlet" amplitude does not contribute to our cross section for the process in Fig. 1.

Turning now to the soft real emission process in Fig. 1(b), we again follow the methods of YFS in [2] and extract the infrared-divergent part of the real gluon bremsstrahlung as

$$d\sigma^{B1}_{\rm soft} = d\sigma_0(2\alpha_s\tilde{B}_{\rm QCD}) \ , \tag{5}$$

where the real QCD infrared function is

$$2\alpha_s\tilde{B}_{\rm QCD} = \int^{k\leq K_{\rm max}} \frac{d^3k}{k_0}\tilde{S}_{\rm QCD}(k) \tag{6}$$

with

$$\begin{aligned}\tilde{S}_{\rm QCD}(k) = -\frac{\alpha_s}{4\pi}\Bigg\{ & C_F\left(\frac{p_1}{p_1\cdot k}-\frac{q_1}{q_1\cdot k}\right)^2 - \Delta C_t\frac{2p_1\cdot q_1}{k\cdot p_1 k\cdot q_1} + C_F\left(\frac{p_2}{p_2\cdot k}-\frac{q_2}{q_2\cdot k}\right)^2 - \Delta C_t\frac{2p_2\cdot q_2}{k\cdot p_2 k\cdot q_2}\\ & + C_F\left(\frac{p_1}{p_1\cdot k}-\frac{p_2}{p_2\cdot k}\right)^2 - \Delta C_s\frac{2p_1\cdot p_2}{k\cdot p_1 k\cdot p_2} + C_F\left(\frac{q_1}{q_1\cdot k}-\frac{q_2}{q_2\cdot k}\right)^2 - \Delta C_s\frac{2q_1\cdot q_2}{k\cdot q_1 k\cdot q_2}\\ & - C_F\left(\frac{q_1}{q_1\cdot k}-\frac{p_2}{p_2\cdot k}\right)^2 + \Delta C_u\frac{2q_1\cdot p_2}{k\cdot q_1 k\cdot p_2} - C_F\left(\frac{q_2}{q_2\cdot k}-\frac{p_1}{p_1\cdot k}\right)^2 + \Delta C_u\frac{2q_2\cdot p_1}{k\cdot q_2 k\cdot p_1}\Bigg\},\end{aligned} \tag{7}$$

where $K_{\rm max}$ corresponds to the relevant gluon jet detector resolution energy ($\sim$ 3 GeV at the LHC) and $k_0 \equiv \sqrt{\vec{k}^2+\lambda^2}$ so that we regulate the infrared singularities in (7) in complete analogy with our gluon mass regulator in (2). [Note that graph (v) in Fig. 1(c) is not infrared divergent.] Here, $d\sigma_0$ is the respective Born differential cross section. The results (1)–(7) represent the complete infrared (IR) structure of QCD for the cross section for $q + \overset{(-)}{q}{}' \to q'' + \overset{(-)}{q}{}''' + (G)$ to order α_s. The result (7) is consistent with the pioneering work of Berends and Giele in [7]. Following the YFS theory, we see that the criterion for the cancellation of the $O(\alpha_s)$ and IR singularities in the cross section for our scattering process in Fig. 1 is that

$$\mathcal{S}_{\rm IR}({\rm QCD}) \equiv 2\alpha_s\tilde{B}_{\rm QCD} + 2\alpha_s{\rm Re}B_{\rm QCD} \tag{8}$$

should be independent of λ. Using the well-known results [2, 8] for the integrals in (2) and (7) (notice that these are just the same integrals that arise in the YFS analysis of QED with different color-based weights) we see that, indeed, λ does cancel out of (8). We are left with the fundamental result (for, e.g., $m_q = m_{q'} = m$)

$$\mathcal{S}_{\rm IR}({\rm QCD}) = \frac{\alpha_s}{\pi}\sum_{A=\{s,t,u,s',t',u'\}}(-1)^{\rho(A)}[C_F B_{\rm tot}(A) + \Delta C_A B'_{\rm tot}(A)] \ , \tag{9}$$

where

$$B_{\rm tot}(A) = \ln(2K_{\rm max}/\sqrt{|A|})^2[\ln(|A|/m^2)-1] + \frac{1}{2}\ln(|A|/m^2) - 1 - \pi^2/6 + \theta(A)\pi^2/2 \quad ,$$

$$B'_{\rm tot}(A) = \ln(2K_{\rm max}/\sqrt{|A|})^2 + \frac{1}{2}\ln(|A|/m^2) - \pi^2/6 + \theta(A)\pi^2/2 \ , \tag{10}$$

and

$$\rho(A) = \begin{cases} 0, & A = s, s', t, t', \\ 1, & A = u, u'. \end{cases} \tag{11}$$

Results (9) and (10) are then the fundamental results of our analysis.

Indeed, repeating the arguments in [2] and/or using the factorization results in [7], we see that by virtue of (9), we may compute the hard gluon radiation residuals at $O(\alpha_s)$ as

$$\bar{\beta}_0 = d\sigma^{\text{one loop}} - 2\alpha_s \text{Re} B_{\text{QCD}} d\sigma_0 \tag{12}$$

and

$$\bar{\beta}_1 = d\sigma^{B1} - \tilde{S}_{\text{QCD}} d\sigma_0 \tag{13}$$

in the exponentiated formula (this formula follows [3] as well from (9), the arguments in [2] and/or the factorization results in Ref. [7], see the Appendix)

$$d\sigma_{\text{exp}} = \exp[\mathcal{S}_{\text{IR}}(\text{QCD})] \sum_{n=0}^{\infty} \frac{1}{n!} \int \prod_{j=1}^{n} \frac{d^3k_j}{k_j} \int \frac{d^4y}{(2\pi)^4} e^{[+iy(p_1+p_2-q_1-q_2-\sum_j k_j)+D]} \bar{\beta}_n(k_1,\ldots,k_n) \frac{d^3q_1 d^3q_2}{q_1^0 q_2^0} , \tag{14}$$

where

$$D = \int \frac{d^3k}{k_0} \tilde{S}_{\text{QCD}} \left[e^{-iy\cdot k} - \theta(K_{\max} - |\vec{k}|) \right] . \tag{15}$$

Here, we use the virtual one-loop correction

$$d\sigma^{\text{one loop}} = d\sigma_0 \delta_{\text{vir}} , \tag{16}$$

where

$$\begin{aligned} \delta_{\text{vir}} = \frac{2\alpha_s}{\pi} \Bigg[& (C_F - \tfrac{1}{2}C_A) \left\{ \ln \frac{|t|}{m^2} \left(2 - \ln \frac{|t|}{\lambda^2} + \frac{1}{2} \ln \frac{|t|}{m^2} \right) \right. \\ & \left. + \ln \frac{s}{m^2} \left(2 \ln \frac{s}{\lambda^2} - \ln \frac{s}{m^2} \right) + \frac{tu}{s^2+u^2} \ln \frac{s}{|t|} \left(\frac{1}{2}(s/u - 1) \ln \frac{s}{|t|} - 1 \right) \right\} \\ & -(C_F - \tfrac{1}{4}C_A) \left\{ \ln \frac{|u|}{m^2} \left(2 \ln \frac{|u|}{\lambda^2} - \ln \frac{|u|}{m^2} \right) + \frac{st}{s^2+u^2} \ln \frac{u}{t} \left(\frac{1}{2}(1 - u/s) \ln \frac{u}{t} - 1 \right) \right\} \\ & + C_F \ln \frac{|t|}{\lambda^2} + C_A \left(\ln \frac{|t|}{m^2} + 1 \right) + \frac{31}{36} C_A - \frac{5}{9} C_F + \frac{\pi^2}{6} C_F \Bigg] . \end{aligned} \tag{17}$$

Here, $C_A = 3$ is the adjoined color-quadratic Casimir invariant. The respective soft real gluon bremsstrahlung cross is given by (5) with

$$\begin{aligned} 2\alpha_s \tilde{B}_{\text{QCD}} = \frac{2\alpha_s}{\pi} \Bigg[& (C_F - \tfrac{1}{2}C_A) \left\{ \ln \frac{4K_{\max}^2}{\lambda^2} + \ln \frac{|t|}{m^2} \left(1 + \ln \frac{4K_{\max}^2}{\lambda^2} - \frac{1}{2} \ln \frac{|t|}{m^2} \right) \right. \\ & \left. -2 \ln \frac{s}{m^2} \left(1 + \ln \frac{4K_{\max}^2}{\lambda^2} - \frac{1}{2} \ln \frac{s}{m^2} \right) \right\} \\ & + (C_F - \tfrac{1}{4}C_A) \left\{ -2 \ln \frac{4K_{\max}^2}{\lambda^2} + 2 \ln \frac{|u|}{m^2} \left(1 + \ln \frac{4K_{\max}^2}{\lambda^2} - \frac{1}{2} \ln \frac{|u|}{m^2} \right) - \frac{\pi^2}{3} \right\} \Bigg] . \end{aligned} \tag{18}$$

It allows $\bar{\beta}_0$ to be identified as $d\sigma_{\text{soft}}^{O(\alpha_s)} - 2\alpha_s(\tilde{B}_{\text{QCD}} + B_{\text{QCD}}) d\sigma_0$, where $d\sigma_{\text{soft}}^{O(\alpha_s)} = d\sigma^{\text{one loop}} + d\sigma_{\text{soft}}^{B1}$, for example. The above expressions are for incoming $q\bar{q}$ and need to be modified accordingly for qq interactions. The hard gluon residual $\bar{\beta}_1$ makes a vanishing contribution in the soft gluon limit so that it will be presented elsewhere [5]; for here we focus on the soft gluon effects in (14) so that we will not need $\bar{\beta}_1$ in the current discussion. We should emphasize that the result (14) in no way contradicts the pioneering work of Marchesini and Webber in [9]. Indeed, the key point in the comparison of our work with that of the latter authors is the comparison of the respective sizes of the infrared cutoffs—in [9] this cutoff is $Q_0 \geq 600$ MeV whereas in our work it is $\lambda \to 0$. Thus, Marchesini and Webber analyze phenomena at or below the scale of the size of a typical hadron radius whereas we analyze true infinite wavelength phenomena. The two analyses therefore deal with complementary regimes of the phase space and, to repeat, in no way contradict one another. In fact, the methods in [9] are a leading candidate for a methodology to calculate the hard gluon residuals $\bar{\beta}_n$ in (14).

The results (12) and (16)–(18) are now realized in (14) via Monte Carlo methods by replacing the QED forms of $\bar{\beta}_n$, $\mathcal{S}_{\text{IR}}$ as described in [1] for our SSCYFS2 and LHCBHL event generators by the respective QCD forms. The resulting event generators are LHCYFSG and LHCBHLG, where in the former, only gluon radiation from the initial state is treated. Sample Monte Carlo data from LHCBHLG are illustrated in the next section. Similar data for

LHCYFSG will appear elsewhere [5].

We should stress that two limits of the QCD coupling constant are needed in (12), (13), and (14). One is the perturbative $-q^2 \gg \Lambda^2_{\rm QCD}$ regime in the hard gluon residuals $\bar{\beta}_n$ in (14). This regime is well known and we use the standard type of formula [10]

$$\alpha_s(\mu) = \frac{12\pi}{(33-2n_f)\ln[\mu^2/(\Lambda^{\overline{\rm MS}}_{n_f})^2]} \tag{19}$$

with n_f the number of open flavors and $\Lambda^{\overline{\rm MS}}_n$ the respective value of $\Lambda_{\rm QCD}$: we take $\Lambda^{\overline{\rm MS}}_4 \simeq 0.238$ GeV for definiteness, where $\overline{\rm MS}$ denotes the modified minimal subtraction scheme.

The second regime occurs in $\mathcal{S}_{\rm IR}$ in (9), where the $k^2 \to 0$ limit is relevant for "on-shell" gluons of four-momentum k. (We follow Tarrah [11] and use the concept of on-shell quarks and gluons in perturbation theory at large momentum transfer.) Recently [12], it has been pointed out by Mattingly and Stevenson that this limit of α_s/π exists as an infrared fixed point and its limiting value is $\simeq 0.263$. We use this value of (α_s/π) in $\mathcal{S}_{\rm IR}$ in (9) and (14). Because of the fixed point behavior, the value one uses for the $k^2 \to 0$ coupling of gluons is not sensitive to the precise value $\Lambda^{\overline{\rm MS}}_4$, for example. Further, since we only work to $O(\alpha_s)$ in the hard interactions, there is no contradiction between our use of $\Lambda^{\overline{\rm MS}}$ values in (19) and the renormalization scheme of Mattingly and Stevenson in [12].

We should also note that our light quark masses are always those determined by Leutwyler and Gaisser in [13]: $m_u(1\ {\rm GeV}) \simeq 5.1 \times 10^{-3}$ GeV, $m_d(1\ {\rm GeV}) \simeq 8.9 \times 10^{-3}$ GeV, $m_s(1\ {\rm GeV}) \simeq 0.175$ GeV, $m_c(1\ {\rm GeV}) \simeq 1.3$ GeV, $m_b(m_b) \simeq 4.5$ GeV; for m_t, we take $m_t(m_t) \simeq 164$ GeV. The running of these masses is readily incorporated into our calculations [13]; we ignore this running in the current paper, since it does not affect our results at the level of accuracy of interest to us here.

With these explanatory remarks in mind, we now turn to explicit Monte Carlo data illustrations for multiple-gluon effects in $q + \overset{(-)}{q}{}' \to q'' + \overset{(-)}{q}{}''' + n(G)$ at LHC energies in the ATLAS and CMS acceptances.

III. RESULTS

In this section, we illustrate our multiple-gluon Monte Carlo event generators in the sample case of $u + u \to u + u + n(G)$, where we require the outgoing u quarks to satisfy $|\eta| \leq 2.8$ and $E > 58$ GeV, for definiteness, at $\sqrt{s} = 15.4$ TeV. (We comment about the case $\sqrt{s} = 40$ TeV as well for pedagogical reasons with an eye toward any possible higher energy collider.) For completeness, we will show explicit Monte Carlo data for LHCBHLG, since in that generator initial, initial-final interference, and final-state $n(G)$ radiation is simulated.

Our results are shown in Figs. 2, 3, and 4, where we show, respectively, the gluon multiplicity, the distribution of $v = (s - s')/s$, where s' is the squared invariant mass of the final quark-quark system, and the total gluon transverse momentum in TeV units. What we see is that there is a pronounced effect from the multigluon radiation at $\sqrt{s} = 15.4$ TeV: the average value of the number of radiated gluons with energy $E_G > 3$ GeV is, e.g., at $\sqrt{s} = 15.4$ TeV,

$$\langle n_G \rangle = 28.5 \pm 5.5. \tag{20}$$

The average value of v is, for $\sqrt{s} = 15.4$ TeV,

$$\langle v \rangle = 0.92 \pm 0.14. \tag{21}$$

The average value of the total transverse momentum in gluons is

$$\langle p_{\perp,{\rm tot}} \rangle \equiv \left\langle \left| \sum_{i=1}^{n} \vec{k}_{i\perp} \right| \right\rangle = (0.19 \pm 0.23)\ {\rm TeV}. \tag{22}$$

This means that a substantial amount of incoming and outgoing energy is radiated into gluons (due to the usual collinearity of radiation with its source, most of the final-state radiation would be a part of the typical jet associated with its parent quark). Entirely similar results hold for the $\sqrt{s} = 40$ TeV case. Evidently, any realistic treatment of QCD corrections to LHC processes must analyze the full event-by-event n-gluon effects as they interact with the detector efficiencies and cuts. Our LHCBHLG event generator provides the first amplitude-based exponentiated Monte Carlo realization of such n-gluon effects and we hope to participate in a study of their interplay with detector effects elsewhere [5].

An important consequence of our work is a prediction for the effect on the overall normalization of an LHC physics process due to multiple–gluon radiation, in an unambiguous way, since all IR-singular effects have canceled out of our calculation. For example, if we simply compute the $O(\alpha_s)$ soft cross section, $E_G < 3$ GeV, we get [for $u + u \to u + u + (G)$, $\sqrt{s} = 40$ TeV] that

$$\sigma/\sigma_{\rm Born} = 1 + \delta_{\rm vir} + \delta_{\rm real} = -22.1, \tag{23}$$

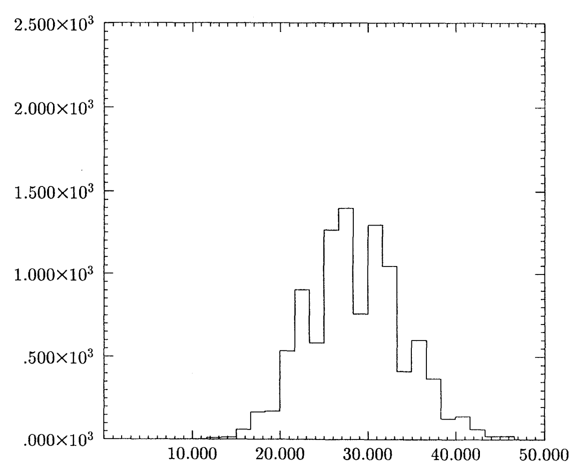

FIG. 2. Gluon multiplicity distribution in $u + u \to u + u + n(G)$ at $\sqrt{s} = 15.4$ TeV.

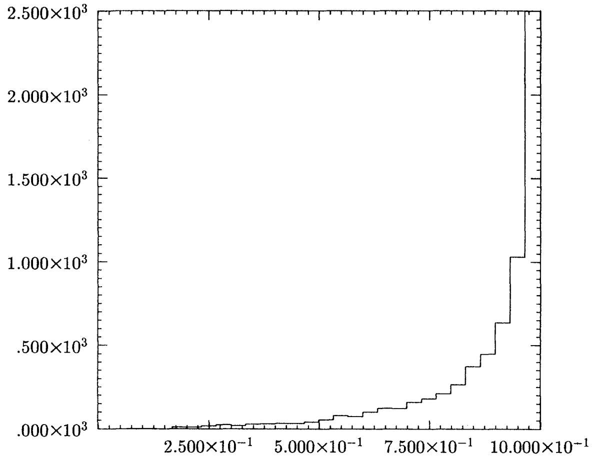

FIG. 3. v distribution in $u+u \to u+u+n(G)$ at $\sqrt{s} = 15.4$ TeV.

whereas if we compute the cross section for $u + u \to u + u + n(G)$ and require $v < 3$ GeV/7.7 TeV= 0.000 39, we get

$$\sigma/\sigma_{\mathrm{Born}} = 1.2 \times 10^{-11}. \tag{24}$$

Hence, we see that multigluon radiation is crucial to getting the proper normalization of the cross section.

We emphasize that the results for $\sqrt{s} = 40$ TeV give similar conclusions [5] to those in Figs. 2–4. Entirely analogous results hold for the pure initial-state multigluon event generator LHCYFSG, except only two lines radiate, so that $\langle n_G \rangle$ is reduced by a factor ~ 2, with the appropriate corresponding reductions in $\langle v \rangle$ and $\langle p_{\perp,\mathrm{tot}} \rangle$. Such results are effectively an integration over the events used in Figs. 2–4, wherein one integrates over all gluons within some cones close to the outgoing fermions. We do not show a separate set of plots for LHCYFSG here but we will present a more detailed discussion of the respective initial-state n-gluon radiation elsewhere [5]. Here, we are focusing on the complete gluon radiation problem.

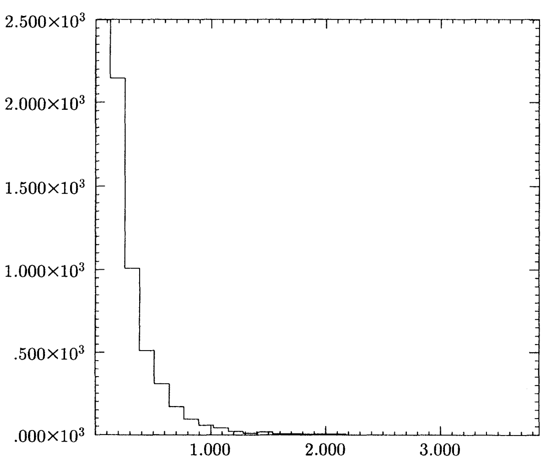

FIG. 4. Total transverse momentum of gluons in $u + u \to u + u + n(G)$ at $\sqrt{s} = 15.4$ TeV. The units of the horizontal axis are TeV.

IV. CONCLUSIONS

In this paper, we have shown that the IR singularities in fermion-(anti)fermion scattering at LHC energies in QCD cancel at order α_s, permitting an immediate extension of YFS QED exponentiation methods to such processes. The YFS Monte Carlo methods invented by two of us [14] (S.J. and B.F.L.W.) for QED radiation in Z^0 physics can then be extended to multigluon Monte Carlo event generators with well-defined IR behavior to all orders in α_s. Such a Monte Carlo realization of amplitude-based n-gluon effects opens the way to a new era in higher-order QCD corrections to hard processes such as those of interest to the LHC physics program.

More specifically, we have realized our exponentiated, n-gluon effects via the Monte Carlo event generators LHCBHLG and LHCYFSG. Since the latter amounts to an initial-state restriction of the former, we have presented results from the former generator in this paper. We find, for example, that the average number of radiated gluons in $u + u \to u + u + n(G)$ at $\sqrt{s} = 15.4$ TeV is 28.5 ± 5.5 and that $\langle v \rangle = 0.92 \pm 0.14$. Further, the cross-section normalization is strongly affected by our n-gluon effects. Hence, only by taking these effects into account, as they interact with detector simulation, for example, can a truly detailed picture of the LHC physics platform be obtained. We hope to participate in such an investigation elsewhere.

In summary, we have presented, for the first time, the realistic event-by-event Monte Carlo realization of multigluon effects in hard QCD processes at LHC energies in which IR singularities are canceled to all orders in α_s. A new approach to LHC physics has thus been created. We look forward with excitement to its many applications.

ACKNOWLEDGMENTS

The authors thank Professor F. Gilman and Professor W. Bardeen for the kind hospitality of the SSCL Theory Department, wherein a part of this work was completed. This research was supported in part by the Texas National Research Laboratory Commission under contracts RCFY9101, RCFY9201, and RCFY-93-347 and by Polish Government grants KBN 20389101 and KBN 223729102.

APPENDIX

In this appendix, we give the essential steps needed to derive the result (14) in the text. We use explicit construction in complete analogy with the original YFS argument itself.

Specifically, we start with the amplitude $\mathcal{M}^{(n)}$ for n-gluon emission in our basic process in Fig. 1, where we may presume color exchange on each fermion line in Fig. 1(a) for definiteness. Using the standard Feynman-Schwinger perturbation series, we may expand $\mathcal{M}^{(n)}$ in the number of virtual gluon loops as a power series in $\frac{\alpha_s}{\pi}$ as usual. The result is

$$\mathcal{M}^{(n)} = \sum_{\ell=0}^{\infty} M_\ell^{(n)}, \tag{A1}$$

where ℓ denotes the number of gluon loops and $M_\ell^{(n)}$ is the contribution to $\mathcal{M}^{(n)}$ with ℓ such loops. Following YFS, we symmetrize $M_\ell^{(n)}$ with the definition

$$M_\ell^{(n)} = \frac{1}{\ell!}\int \prod_{j=1}^{\ell} \frac{d^4k_j}{(2\pi)^4(k_j^2 - \lambda^2 + i\epsilon)} \rho_\ell^{(n)}(k_1,\ldots,k_\ell), \tag{A2}$$

where this serves to define $\rho_\ell^{(n)}$ as a symmetric function of its gluon-loop momentum arguments k_j. Suppose now that k_ℓ approaches the infrared point $O = (0,0,0,0)$ while all other k_j are fixed away from O. Then, we showed in the text that we must get, for any one-loop amplitude for gluon ℓ,

$$\rho_\ell^{(n)} = S(k_\ell) * \rho_{\ell-1}^{(n)}(k_1,\ldots,k_{\ell-1}) + \beta_\ell^1(k_1,\ldots,k_{\ell-1};k_\ell), \tag{A3}$$

where $S(k)$ is α_s times the integrand of $B_{\rm QCD}$ in (2) with a factor of $1/[(2\pi)^4(k^2 - \lambda^2 + i\epsilon)]$ removed and $\beta_\ell^1(k_1,\ldots,k_{\ell-1};k_\ell)$ is not infrared divergent in k_ℓ by our one-loop analysis in the text. We now use the symmetry of $\rho_\ell^{(n)}$ for all n,ℓ to conclude that (A3) implies

$$\begin{aligned}\rho_\ell^{(n)} = {} & S(k_\ell)S(k_{\ell-1}) * \rho_{\ell-2}^{(n)}(k_1,\ldots,k_{\ell-2}) \\ & +S(k_\ell)\beta_{\ell-1}^1(k_1,\ldots,k_{\ell-2};k_{\ell-1}) \\ & +S(k_{\ell-1})\beta_{\ell-1}^1(k_1,\ldots,k_{\ell-2};k_\ell) \\ & +\beta_\ell^2(k_1,\ldots,k_{\ell-2};k_{\ell-1},k_\ell),\end{aligned} \tag{A4}$$

where, now, β_ℓ^2 is not infrared divergent in the two arguments $k_\ell, k_{\ell-1}$ and is also a symmetric function of these arguments. Applying (A4) repeatedly, we get finally the usual YFS representation

$$\begin{aligned}\rho_\ell^{(n)} = {} & S(k_1)\ldots S(k_\ell)\beta_0 + \sum_{i=1}^{\ell}\prod_{j\neq i} S(k_j)\beta_1(k_i) \\ & +\cdots+\beta_\ell(k_1,\ldots,k_\ell),\end{aligned} \tag{A5}$$

where we have defined the virtual gluon residuals $\beta_i(k_1',\ldots,k_i')$ which are free of virtual infrared singularities in $k_j', j=1,\ldots,i$. In the standard YFS notation, β_i are just the residuals β_i^i implied in the repeated application of (A3) and (A4). Upon introducing (A5) into (A1), we get the familiar result [2]

$$\mathcal{M}^{(n)} = \exp(\alpha_s B_{\rm QCD}) \sum_{j=0}^{\infty} m_j^{(n)}, \tag{A6}$$

where $B_{\rm QCD}$ is given in the text and here we now have

$$m_j^{(n)} = \frac{1}{j!}\int \prod_{i=1}^{j} \frac{d^4k_i}{k_i^2}\beta_j(k_1,\ldots,k_j), \tag{A7}$$

as usual. The important point is that, since we integrate over the entire four-volume of k space for each gluon, even though the color algebra may have both symmetric and antisymmetric terms under exchange of gluon i and gluon j, the k-space dependence of $\rho^{(n)}$ for each gluon must be symmetric in the exchange of any two gluons in order to contribute to the multiple-loop integration.

Turning now to the real gluon soft emission formulas, we note that the differential cross section for the emission of n soft gluons with total energy ϵ has the form

$$d\sigma^n/d\epsilon = \exp(2\alpha_s {\rm Re} B_{\rm QCD})\frac{1}{n!}\int \prod_{m=1}^{n} \frac{d^3k_m}{(k_m^2+\lambda^2)^{1/2}}\delta\left(\epsilon - \sum_{i=1}^{n} k_i^0\right)\bar{\rho}^{(n)}(p_1,p_2,q_1,q_2,k_1,\ldots,k_n)\ , \tag{A8}$$

where the $\bar{\rho}^{(n)}$ are given by the standard phase space factor times the modulus squared of $\sum m_i^{(n)}$ as usual. We may again use the same procedure as we did in the virtual case to remove the infrared divergent contributions due to real emission from the function $\bar{\rho}^{(n)}(k_1,\ldots,k_n)$, where again we exploit the symmetry of $\bar{\rho}^{(n)}$ in its arguments and our known result for the infrared factor associated with the emission of one real soft gluon as given in the text by $\tilde{S}_{\rm QCD}$ in (7). We get

$$\begin{aligned}\bar{\rho}^{(n)}(k_1,\ldots,k_n) = {} & \tilde{S}_{\rm QCD}(k_1)\cdots\tilde{S}_{\rm QCD}(k_n)\bar{\beta}_0 + \sum_{i=1}^{n}\tilde{S}_{\rm QCD}(k_1)\cdots\tilde{S}_{\rm QCD}(k_{i-1})\tilde{S}_{\rm QCD}(k_{i+1})\cdots\tilde{S}_{\rm QCD}(k_n)\bar{\beta}_1(k_i) + \cdots \\ & +\sum_{i=1}^{n}\tilde{S}_{\rm QCD}(k_i)\bar{\beta}_{n-1}(k_1,\ldots,k_{i-1},k_{i+1},\ldots,k_n) + \bar{\beta}_n(k_1,\ldots,k_n),\end{aligned} \tag{A9}$$

where all infrared divergences are contained in the products of the $\tilde{S}_{\rm QCD}$ and the $\bar{\beta}_j$ are infrared divergence free. On introducing the result (A9) into (A8) and summing (A8) over n, we get the result (14) in the text, using the standard YFS manipulations illustrated for the virtual case. We stress again that, as in the virtual case, the symmetry of the n-gluon phase space integration allows us to symmetrize $\bar{\rho}^{(n)}$ in its n-gluon momentum arguments and thus allows us to carry through the YFS real gluon exponentiation procedure in the infrared regime. This completes our appendix.

[1] D. B. DeLaney *et al.*, Phys. Rev. D **47**, 853 (1993).
[2] D. R. Yennie, S. C. Frautschi, and H. Suura, Ann. Phys. (N.Y.) **13**, 379 (1961).
[3] D. B. DeLaney *et al.*, Phys. Lett. B **342**, 239 (1995).
[4] S. Jadach, E. Richter-Was, B. F. L. Ward, and Z. Was, Comput. Phys. Commun. **70**, 305 (1992).
[5] D. B. DeLaney *et al.* (unpublished).
[6] J. M. Cornwall, Phys. Rev. D **10**, 500 (1974).
[7] F. A. Berends and W. T. Giele, Nucl. Phys. **B313**, 595 (1989).
[8] B. F. L. Ward, Phys. Rev. D **36**, 939 (1987); **42**, 3249 (1990).
[9] G. Marchesini and B. R. Webber, Nucl. Phys. **B310**, 461 (1988).
[10] D. J. Gross and F. Wilczek, Phys. Rev. Lett. **30**, 1343 (1973); H. D. Politzer, *ibid.* **30**, 1346 (1973); G. 't Hooft (unpublished).
[11] R. Tarrah, Nucl. Phys. **B183**, 384 (1981).
[12] A. C. Mattingly and P. M. Stevenson, Phys. Rev. Lett. **69**, 1320 (1992).
[13] J. Gaesser and H. Leutwyler, Phys. Rep. **87**, 77 (1982); see also S. Weinberg, in *Festschrift for I. I. Rabi*, edited by L. Motz (New York Academy of Sciences, New York, 1977).
[14] S. Jadach and B. F. L. Ward, Comput. Phys. Commun. **56**, 351 (1990), and references therein.